Gadolinium-sensitive, voltage-dependent calcium release channels in the endoplasmic reticulum of a higher plant mechanoreceptor organ

Birgit Klüsener[1,2], Günther Boheim[2], Harald Liß[1], Jürgen Engelberth[1] and Elmar W.Weiler[1,3]

[1]Department of Plant Physiology and [2]Biophysical Chemistry of Membranes Group, Ruhr-University, D-44780 Bochum, Germany

[3]Corresponding author

The lipid bilayer technique was adapted to the functional reconstitution of ion channels from the endoplasmic reticulum of a higher plant. This was obtained at high purity from touch-sensitive tendrils of *Bryonia dioica*. In this preparation, a calcium-selective strongly rectifying channel is prevailing whose single-channel properties have been characterized. The single-channel conductance is 29 pS in 50 mM $CaCl_2$. The Ca^{2+}:K^+ selectivity was determined to be ~6.6. The channel is voltage-gated and, more importantly, the gating voltage is strongly shifted towards more negative voltages when a transmembrane Ca^{2+} gradient is applied. Thus, at physiological voltages across the endoplasmic reticulum membrane, the channel's open probability will be governed largely by the chemical potential gradient of Ca^{2+}, generated by the Ca^{2+}-ATPase in that same membrane. The calcium release channel described here is effectively blocked by Gd^{3+} which also completely suppresses a tendril's reaction to touch, suggesting that this channel could be a key element of calcium signaling in higher plant mechanotransduction. Its molecular characteristics and inhibitor data show it to be the first known member of a hitherto unrecognized class of calcium channels.

Key words: calcium channels/calcium oscillator/endoplasmic reticulum/mechanotransduction/signal transduction

Introduction

Calcium is by now well recognized as an important regulatory element in the transduction of exogenous (environmental or pathogenic) as well as endogenous (hormonal) signals in plant cells (Leonard and Hepler, 1990). Transient changes in the level of cytoplasmic calcium have been associated with the reactions of plants to such diverse factors as touch and wind force, light, cold-shock or elicitation (Knight *et al.*, 1991, 1992). Two major pathways for the delivery of calcium to the cytosol have been postulated, namely (i) entry from the extracellular fluid (Schroeder and Hagiwara, 1990; Thuleau *et al.*, 1994) and/or (ii) release from internal stores (Gilroy *et al.*, 1991; Knight *et al.*, 1991, 1992), and it appears that different stimuli utilize different pools of calcium (Knight *et al.*, 1991, 1992). Work on transgenic tobacco

expressing cytosolic apoaequorin has shown that touch or wind force produce transient rises in cytosolic free calcium in this species which are insensitive to apoplastic Gd^{3+} and are thus fed from internal calcium stores (Knight *et al.*, 1991, 1992). While vacuolar calcium-conducting channels from plant cells became known recently from patch–clamp studies (Allen and Sanders, 1994; Ward and Schroeder, 1994), no direct demonstration for the existence of calcium channels (ion channels in general) in plant endoplasmic reticulum (ER) membranes is available. Consequently, the properties of such channels are not known.

While a basic reactivity to touch may be a property of any plant cell (Braam and Davis, 1990), reflecting the fact that all plants throughout their life cycle are continuously exposed to mechanical forces and will react to them (by, for example, thigmomorphogenic processes), many plant species have evolved organs geared to the perception of touch. These are the winding and climbing plants, among which the tendril-bearing species are most suited for the study of mechanotransduction because of their high sensitivity towards the stimulus and because of their short reaction times. Tendrils are also ideal experimental systems for the molecular analysis of calcium release from endomembrane stores, especially the ER, as large amounts of pure ER may be produced from them (Liß and Weiler, 1994). Furthermore, the study of tendrils of *Bryonia dioica* has recently yielded detailed information on many aspects of organ function related to mechanotransduction, including primary active calcium transporters (Liß and Weiler, 1994) and the involvement of the prostaglandin-like, cyclic 12-oxo-octadecanoic acids as a novel class of signaling molecules that serve to coordinate the growth reactions of the stimulated organ (Falkenstein *et al.*, 1991; Weiler *et al.*, 1993, 1994) downstream of a calcium signal.

Here, we describe the characteristics of the first discovered plant ER channel, a calcium-selective, gadolinium-sensitive and voltage-gated rectifier channel operated through the transmembrane chemical potential gradient of Ca^{2+} at the single channel level, and propose a working model on its role in mechanotransduction.

Results

In the search for inhibitors of tendril coiling, we observed that Gd^{3+} ions completely abolished the response to touch. While an inhibition of plasma membrane calcium influx systems in both animal (Yang and Sachs, 1989; Lacampagne *et al.*, 1994) and plant cells (Knight *et al.*, 1992; Allen and Sanders, 1994) requires only micromolar levels of extracellular Gd^{3+}, these were ineffective on tendrils. Likewise, the reduction of apoplastic levels of calcium by EGTA did not abolish or diminish the organ's reaction to touch (data not shown). Calcium entry from extracellular sites was therefore not essential for the touch

response. However, at higher levels (Figure 1A) Gd^{3+} was strongly inhibitory, suggesting that the blocker did act on some intracellular location. While patch–clamp analysis of the plasma membrane and tonoplast membrane from different cell types from tendril tissue gave evidence for a repertoire of diverse ion channels (B.Klüsener *et al.*, manuscript in preparation), no indications for calcium-selective channels were obtained at this level of analysis. At the same time it became apparent that while primary
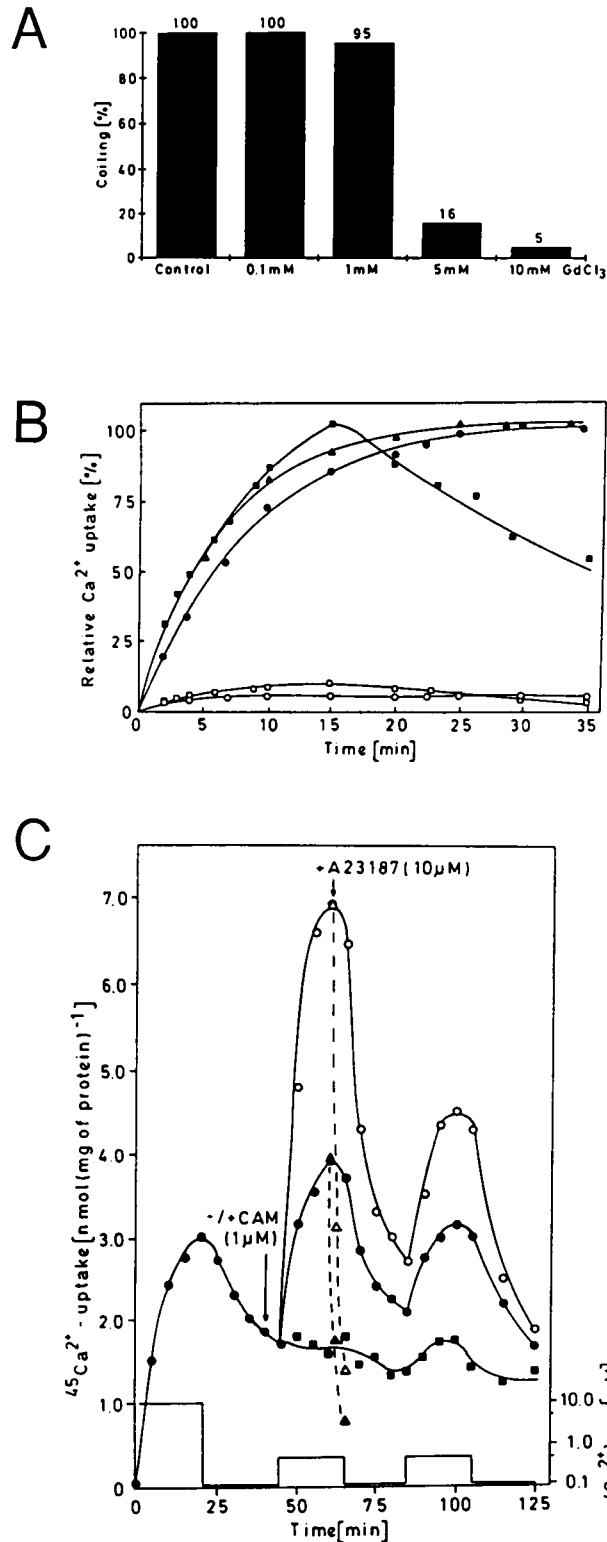
active Ca^{2+} pumps were located at the plasma membrane as well as different endomembranes, the major activity was associated with the ER from tendril tissue (Liß and Weiler, 1994), and this enzyme was calmodulin-regulated. When sealed plasma membrane or ER vesicles were loaded with $^{45}Ca^{2+}$ by the action of the Ca^{2+}-ATPase, both types of vesicle accumulated Ca^{2+} driven by ATP hydrolysis. However, this loading induced a Ca^{2+} efflux in the ER preparations, while no such efflux occurred from plasma membrane vesicles. The Ca^{2+} efflux from the ER was inhibited completely by 20 µM (intravesicular) $GdCl_3$ (Figure 1B). This efflux could not be attributed to leakiness of the ER vesicles, because shifting the extravesicular concentration of Ca^{2+} between 0.1 and 0.5 µM repeatedly led to several cycles of Ca^{2+} uptake (when the extravesicular concentration was stepped up from 0.1 to 0.5 µM) and Ca^{2+} release (when the extravesicular concentration of Ca^{2+} was stepped down from 0.5 to 0.1 µM). The uptake system remained stimulated by calmodulin during the course of the experiment (Figure 1C). These initial observations suggested that in tendrils the ER is a major cellular site of regulated calcium translocation, making this organ well suited for the molecular analysis of these processes. Our study deals with the identification and characterization, at the molecular level, of the ER calcium efflux system.

Since patch–clamping of the ER is impossible, we applied the technique of planar lipid bilayers (Boheim *et al.*, 1981; Hanke *et al.*, 1984) to analyse our membrane preparations by direct reconstitution of proteins from ER vesicles in bilayers formed from a solution of 1-palmitoyl-2-oleoyl-glycero-3-phosphatidylcholine and 1,2-dioleoyl-glycero-phosphatidylethanolamine in *n*-decane. The incorporation of the transport system into the bilayer in the presence of symmetrical 50 mM $CaCl_2$ and the application of a sufficiently high voltage led to the appearance of discrete current fluctuations typical of an ion channel (Figure 2). Since the same conductance value and kinetic behavior were also observed when working with $Ca(NO_3)_2$ or hemi-Ca gluconate, the channel conducts calcium ions. Channel activity occurred in bursts (Figure 2A). When in its active state, an abrupt sign reversal of

Fig. 1. (A) Gd^{3+} inhibits tendril coiling in *B.dioica*. Shoot tips from established plants were placed in $GdCl_3$ dissolved in water (controls, water) and allowed to transpire for 16 h prior to mechanical stimulation (Weiler *et al.*, 1993; Liß and Weiler, 1994) before coiling was scored. (B) $^{45}Ca^{2+}$ loading of sealed plasma membrane (○,●) or ER (□,■) vesicles from tendril tissue in the absence (open symbols) or presence (closed symbols) of 3 mM Mg-ATP. $^{45}Ca^{2+}$ loading of ER vesicles in the presence of ~20 µM intravesicular $GdCl_3$ (▲). $^{45}Ca^{2+}$ uptake: 100% = 20 nmol $^{45}Ca^{2+}$/mg protein (○,●), 7.5 nmol $^{45}Ca^{2+}$/mg protein (□,■) and 9 nmol $^{45}Ca^{2+}$/mg protein (▲).
(C) Repetitive $^{45}Ca^{2+}$ loading and release of $^{45}Ca^{2+}$ from ER vesicles as a function of the concentration of extravesicular free calcium. The initial loading was performed exactly as in (B). At peak levels of intravesicular $^{45}Ca^{2+}$, extravesicular $^{45}Ca^{2+}$ was readjusted to 0.1 µM by the addition of EGTA. At the times indicated, the concentration of free Ca^{2+} was raised to 0.5 µM by the addition of $^{45}Ca^{2+}$ and so on, as shown by the bars above the abscissa. Intravesicular $^{45}Ca^{2+}$ in the absence (●) or presence (○) of calmodulin (CAM, added at the time indicated by the arrow). $^{45}Ca^{2+}$ efflux from untreated control vesicles receiving only the first treatment (at t = 20 min) of EGTA to lower extravesicular free calcium to 0.1 µM (■). $^{45}Ca^{2+}$ release induced by the addition of the calcium ionophore A23187 to vesicles in the presence (△) or absence (▲) of calmodulin to demonstrate exchangeability of vesicle-associated $^{45}Ca^{2+}$.

the membrane voltage rendered the channel completely and instantaneously silent. Returning to the original voltage polarity caused a rapid recovery to the previously observed channel activity (Figure 2B). BCC1 (for *Bryonia* calcium channel 1) is obviously strongly rectifying. Open-state current–voltage relationships derived from single-channel recordings could thus be observed for either positive or
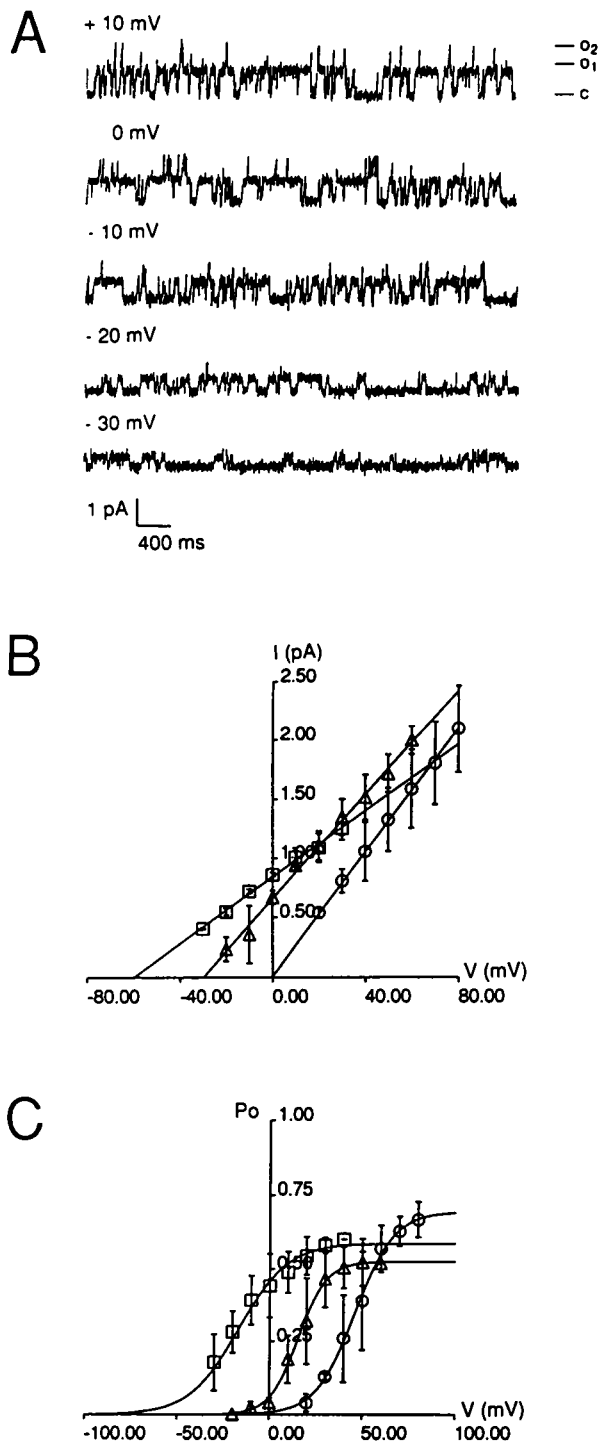

negative voltages, depending on the orientation of the channel in the bilayer in each given experiment (Figure 2C). Data indicate the random distribution of channel insertion into the bilayer. Irrespective of this orientation, the single channel conductance for Ca^{2+} was determined to be 29.0 ± 5.4 pS ($n = 38$). While the channel passes Ba^{2+} slightly better than Ca^{2+} ($\Lambda_{Ba} = 31$ pS), its permeability for Mg ($\Lambda_{Mg} = 6.9$ pS) and alkali ions is much lower. Channel conductances in electrolytes containing $CaCl_2$ and $MgCl_2$ show a small, but significant, anomalous mole fraction effect. From biionic potential measurements (Hille, 1992), a permeability ratio of $P_{Ca^{2+}}/P_{K^+} = 6.6$ was determined, comparable with that observed for Ca^{2+} release channels from animal endomembranes such as the IP_3 and ryanodine receptor channels (Lee and Tsien, 1984) and also to the selectivities of plant plasma membrane or tonoplast calcium channels (Pantoja *et al.*, 1992; Ping *et al.*, 1992; Ding and Pickard, 1993; Allen and Sanders, 1994). From the general assumptions of constant field theory and assuming no difference between internal and external surface potential, the selectivity coefficient is represented by $P_{Ca^{2+}}/P_{K^+} = a_{K^+\ trans}/4a_{Ca^{2+}\ cis} \cdot (1 + e^{-V_{rev}F/RT}) \cdot e^{-V_{rev}F/RT}$ (Lee and Tsien, 1984). For 100 mM KCl and 50 mM $CaCl_2$ electrolyte concentrations, respectively, we determined $V_{rev} = -25$ mV at 298 K (Figure 2D). If we take into consideration the corresponding (molal) ion activities $a_{K^+} = 77.1$ mM and $a_{Ca^{2+}} = 29.5$ mM (D'Ans and Lax, 1967), then $P_{Ca^{2+}}/P_{K^+} = 6.6$.

BCC1 is voltage-gated (Figure 3). Single-channel conductance as well as open-state probability depend strongly on transmembrane differences in Ca^{2+} concentration. P_o is shifted towards more negative membrane voltages when the concentration gradient of Ca^{2+} increases (cf. Figure 3B and C). BCC1 reaches a high open-state probability ($P_o = 0.5$) even at zero applied voltage in a 50 mM/0.5 mM Ca^{2+} gradient. The characteristic values of conductances Λ, formal gating charges α, half saturation voltages $V_{1/2}$ (gating voltage) and reversal potentials V_{rev} are listed in Table I.

Several di- and trivalent ions in low concentrations blocked calcium passage through BCC1: Gd^{3+} ($I_{50} = 1.1$ μM, $n = 5$), Cu^{2+} (1.2 μM, $n = 3$), La^{3+} (9.0 μM, $n = 3$) and Cd^{2+} (100 μM, $n = 3$). Gd^{3+} blocked only when present at the Ca^{2+} entry side of the channel (addition of $GdCl_3$ to the *cis* compartment), while showing no effect when present at the Ca^{2+} exit (*trans*) side. Thus, the ion probably gains access to the calcium entrance of
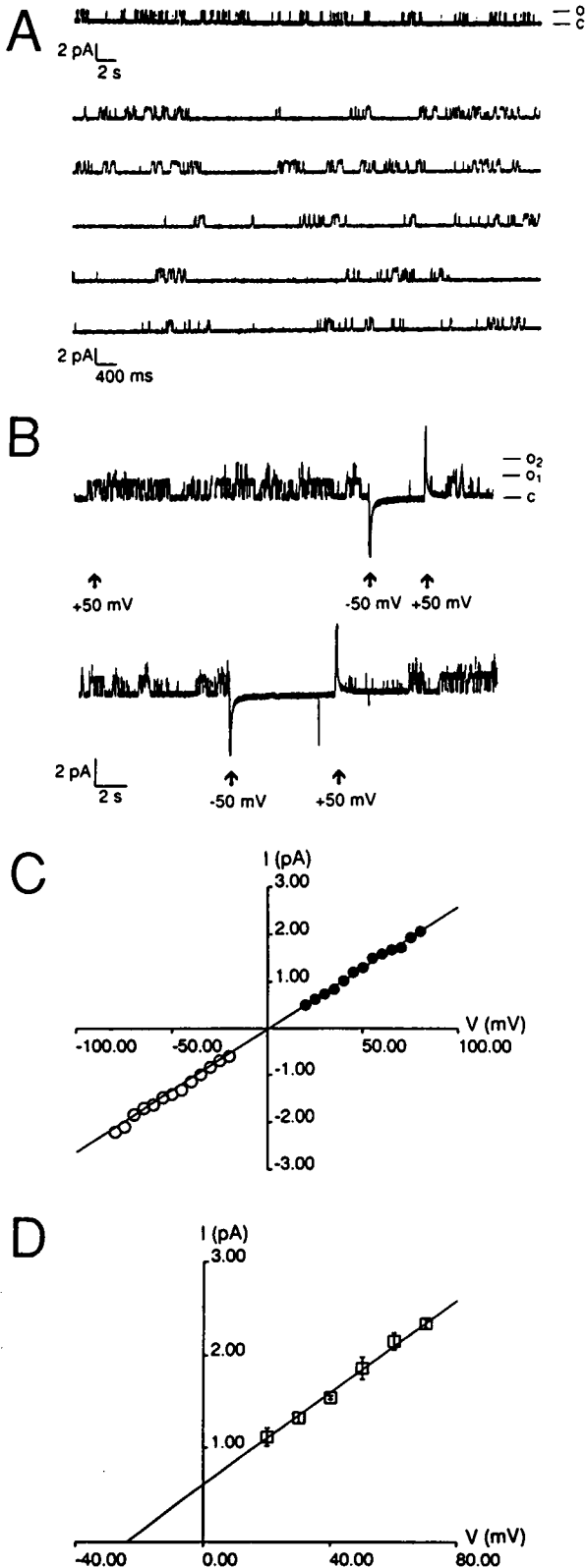
Fig. 2. General characteristics of BCC1. (**A**) Typical current fluctuations of the ER Ca^{2+} channel reconstituted in a planar lipid bilayer in symmetrical 50 mM $CaCl_2$ recorded at +50 mV and shown on a compressed (upper trace) and extended (lower trace) time scale to visualize bursting activity of the channel. (**B**) Rectifying properties of the ER Ca^{2+} channel. At the times shown, the membrane voltage was switched between +50 and −50 mV. Channel activity in this case was seen only when positive voltage was applied to the membrane.

(**C**) Current–voltage relationship of the ER Ca^{2+} channel. Depending on the orientation of the reconstituted and strongly rectifying channel in the bilayer, channel activity could be observed when either positive (●, $\Lambda = 29.2 \pm 6.0$ pS; $n = 21$) or negative voltages (○, $\Lambda = 29.0 \pm 4.5$ pS; $n = 17$) were applied. (**D**) Reversal potential of the ER Ca^{2+} channel under biionic conditions ($n = 3$). V_{rev} was determined by extrapolation of the single-channel current–voltage curve to the zero current axis. Salt concentrations: *cis*, 50 mM $CaCl_2$, 10 mM HEPES, pH 7.0; *trans*, 100 mM KCl, 10 mM HEPES, pH 7.0.

Table I. BCC1 characteristics affected by transmembrane calcium gradients

Ca^{2+} gradient	Λ (pS)	α	$V_{1/2}$ (mV)	V_{rev} (mV)	n
50 mM/50 mM	29.0 ± 5.4	2.4	+46.2	0.0	3
50 mM/5.0 mM	23.6 ± 4.0	3.3	+15.7	−31.0 ± 2.0	3
50 mM/0.5 mM	14.4 ± 1.3	1.9	−16.6	−58.3 ± 1.5	3

Measured mean values of conductance Λ, formal gating charges α, half saturation voltages $V_{1/2}$ (gating voltage) and reversal potentials V_{rev} under various conditions of calcium gradients (calculated from the data shown in Figure 2D; n, number of experiments). The equation used was: $P_o = P_{omax} \cdot 1/[1 + e^{-a(V - V_{1/2})}]$, where $a = \alpha F/RT$, F = Faraday's constant, R = gas constant, T = absolute temperature, V = applied voltage. We set $P_{omin} = 0$.
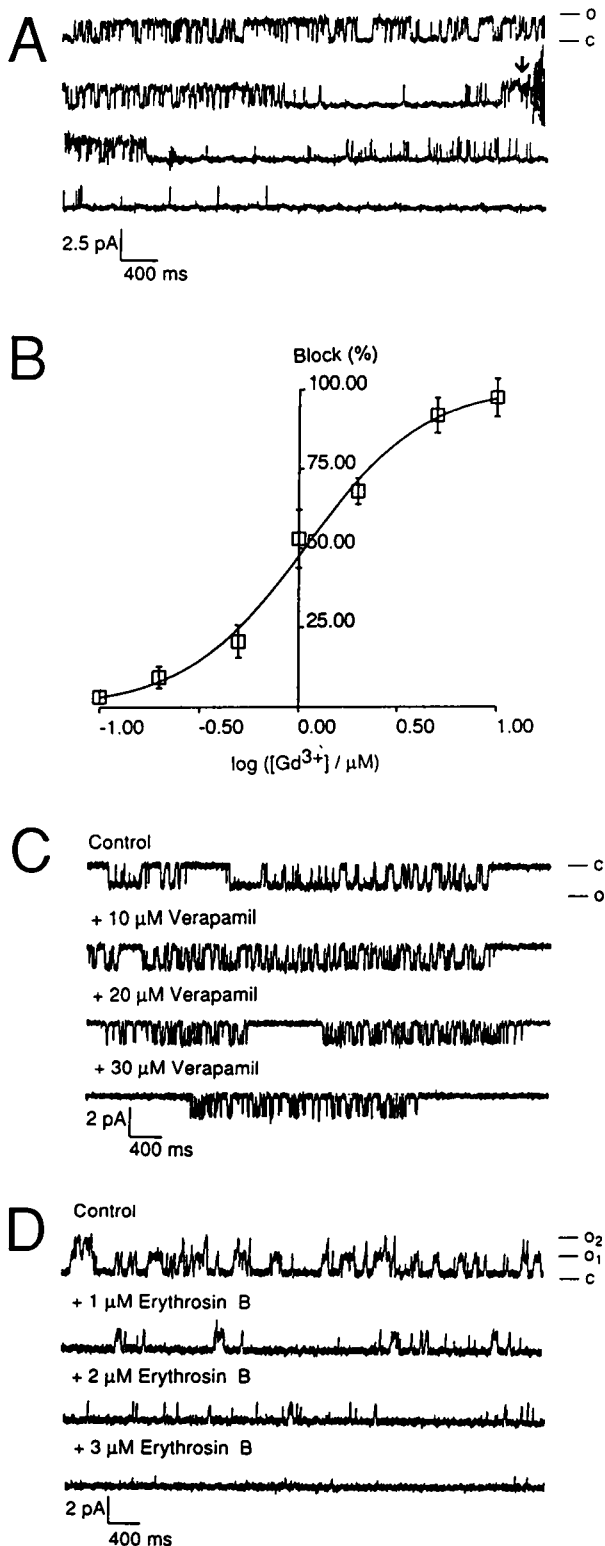
the open channel, leading to obstruction (Hille, 1992). With BCC1 in a state of high open probability, permeation block became apparent on average ~30–60 s after adding Gd^{3+} (10 µM) to the cis compartment (Figure 4A). An almost complete block ($P_o < 0.01$) was reached at ~10 µM and the beginning of P_o reduction at ~0.1 µM Gd^{3+} (Figure 4B).

The 1,4-dihydropyridines nifedipine (≤70 µM) or Bay K 8644 (≤30 µM) did not block BCC1 activity. Interestingly, the phenylalkylamine verapamil has two effects: (i) open-state events within bursts are reduced in mean lifetime, and (ii) the channel's bursting behavior is augmented such that the burst intervals lasting for several seconds were followed by intervals of similar duration exhibiting almost no activity (Figure 4C). BCC1 was unaffected by IP_3 (≤10 µM), ryanodine (≤30 µM), the Ca^{2+}-ATPase inhibitor thapsigargin (≤20 µM), the calmodulin antagonist trifluoperazine (≤40 µM) or by the addition of ADP or ATP (≤2 mM), but was inhibited effectively by erythrosine B (Figure 4D; $I_{50} = 1$ µM). In the light of these data, it becomes clear that the Gd^{3+}-sensitive ER calcium channel from Bryonia tendrils represents a class hitherto unrecognized. It resembles somewhat the neuronal high voltage activated (HVA) L- and N-type calcium channels (Hille, 1992), but it also shows several properties distinctly different from them.

Discussion

The data reported herein prove the presence of ER calcium channels in plants and suggest a major role for them in calcium signaling. Only one type of calcium channel was detected under the specified conditions. BCC1 is fairly calcium-selective, strongly rectifying and exhibits a pronounced voltage dependence of its open-state probability. More positive to ~20 mV and saturating at 80–90 mV, under conditions of symmetrical 50 mM $CaCl_2$ the channel's open-state probability increases steeply. The voltage across the plant ER is not known; however, from data available for the sarcoplasmic reticulum (SR) membrane potential in skeletal muscle (Stephenson et al., 1981; Meissner, 1983) and for the ER of COS cells (Kendall et al., 1992), it can be assumed to be ~12–25 mV with little variation around this basic value (Jafri and Gillo, 1994). Voltage gating of BCC1 under such premises would be useless, and no indications of ligand gating (by IP_3, for example) have been obtained in our experiments. It was then found (cf. Figure 3B and C and Table I) that

Fig. 3. Characteristics of the BCC1 channel under three different Ca^{2+} gradient conditions. (A) Channel current fluctuation traces at various voltages applying the following Ca^{2+} gradient: cis, 50 mM $CaCl_2$, 10 mM HEPES, pH 7.0; trans, 0.5 mM $CaCl_2$, 99.0 mM choline chloride, 10 mM HEPES, pH 7.0. (B) Single-channel current–voltage relationship and (C) voltage dependence of the open-state probability P_o of the ER Ca^{2+} channel. Shown are data from bilayer experiments using three different sets of Ca^{2+} gradients (cis/trans): (i) 50 mM $CaCl_2$ on both sides (○), (ii) 50 mM $CaCl_2/5$ mM $CaCl_2$ + 90 mM choline chloride (△), (iii) 50 mM $CaCl_2/0.5$ mM $CaCl_2$ + 99.0 mM choline chloride (□). Notice the shift of the characteristic gating voltage $V_{1/2}$ towards more negative voltages while lowering trans-side Ca^{2+} concentration.

the gating voltage of BCC1 was shifted strongly towards negative voltages upon the installation of a transmembrane calcium gradient (such as would result from the action of the ER Ca^{2+}-ATPase). In a 10:1 gradient, a 50% open channel probability is reached at ~16 mV; in a 100:1 gradient this value is reached already at approximately −17 mV (see Table I). Again, concentrations of Ca^{2+} in the ER lumen of plants are unknown, but data for other cells suggest a 5- to 20-fold concentration difference

2.5 pA

400 ms

Block (%)

100.00

75.00

50.00

25.00

-1.00   -0.50   0.00   0.50   1.00

log ([Gd^{3+}] / μM)

Control

+ 10 μM Verapamil

+ 20 μM Verapamil

+ 30 μM Verapamil

2 pA

400 ms

Control

+ 1 μM Erythrosin B

+ 2 μM Erythrosin B

+ 3 μM Erythrosin B

2 pA

400 ms

between the cytoplasm and the ER lumen, where the free calcium concentration may reach 5 μM (Kendall *et al.*, 1992; Jafri and Gillo, 1994). Those ratios of Ca^{2+} concentration across the ER membrane would shift the gating voltage $V_{1/2}$ of BCC1 sufficiently towards the negative to result in channel opening.

Although bilayer experiments do not permit the determination of absolute channel orientation, the data shown in Figures 1 and 2 allow only one physiologically meaningful orientation of BCC1 in the ER membrane. This is to allow the passage of calcium ions from the ER lumen into the cytoplasm, while the calmodulin-stimulated Ca^{2+} pump resident in that same membrane has been shown to operate in the opposite direction (Liß and Weiler, 1994). The total block by Gd^{3+} of the tendril's response to touch (cf. Figure 1A) suggests that BCC1 is a key and early element in the signal transduction chain operating in this plant mechanoreceptor organ. Gd^{3+} is a blocker of stretch-activated (SA) channels (Yang and Sachs, 1989). It has been shown to block other channels too, such as the L-type calcium channels in isolated ventricular myocytes (Lacampagne *et al.*, 1994), has several sites of action (Elinder and Århem, 1994) and can thus not be regarded as selective for SA channels. Whether or not BCC1 responds directly to mechanical force is currently unknown. While such a property would directly couple its activity to the mechanoperception event, alternative functional models need to be considered likewise. For example, it is still a mystery as to how the tendril discriminates a rough from a smooth surface and how it discriminates sliding along a support from other kinds of mechanical stress such as hits by raindrops or direct pressure. The organ obviously perceives touch as a pattern in space and time. Several of the properties of BCC1 make it a relevant candidate in this process according to the following working model (Figure 5). Irrespective of changes in the ER membrane potential difference, which is actually unknown and may be assumed to be close to zero (see above), a Ca^{2+} oscillator is proposed. The energy to establish such a dissipative structure is provided by the calmodulin-stimulated Ca^{2+}-ATPase, which pumps Ca^{2+} from the cytoplasm into the ER lumen (Liß and Weiler, 1994). We begin our considerations with the situation that the Ca^{2+} concentration $[Ca^{2+}]_{lum}$ of the ER lumen has

Fig. 4. Inhibitors and modifiers of BCC1 activity. (**A**) Gd^{3+} blocks the activity of the ER Ca^{2+} channel. Shown is a typical single-channel recording obtained in symmetrical 50 mM $CaCl_2$ at an applied voltage of +50 mV. At the time indicated by the arrow, 10 μM $GdCl_3$ were added to the *cis* compartment. The electrolyte was then stirred for 30 s and recordings resumed thereafter (following two traces). The addition of $GdCl_3$ (≤10 mM) to the *trans* compartment had no detectable effect on BCC1 activity. (**B**) Dose–response relationship (*n* = 5) for the channel blockade by Gd^{3+}. Block (%) is defined as 100 · (1 − P_{oa}/P_{ob}), with P_{oa} and P_{ob} being the single-channel open-state probabilities after and before the addition of Gd^{3+}, respectively. (**C**) Effect of verapamil on the kinetic properties of the ER Ca^{2+} channel. Verapamil was added to the *trans* compartment and the solution stirred for 30 s prior to electrical recording. Traces from typical recordings are shown (sidedness definition as given in Materials and methods; but here channel openings appear as downward deflections to indicate the fact that the respective channel was inversely oriented). The *cis*-side addition of verapamil caused a similar but less pronounced effect. (**D**) Erythrosine B, given to the *trans* compartment, reduces open-state probability of the ER Ca^{2+} channel. Comparable with verapamil, the *cis*-side addition of erythrosine B caused a similar but less pronounced effect. Other experimental conditions in (C) and (D) as in (A).
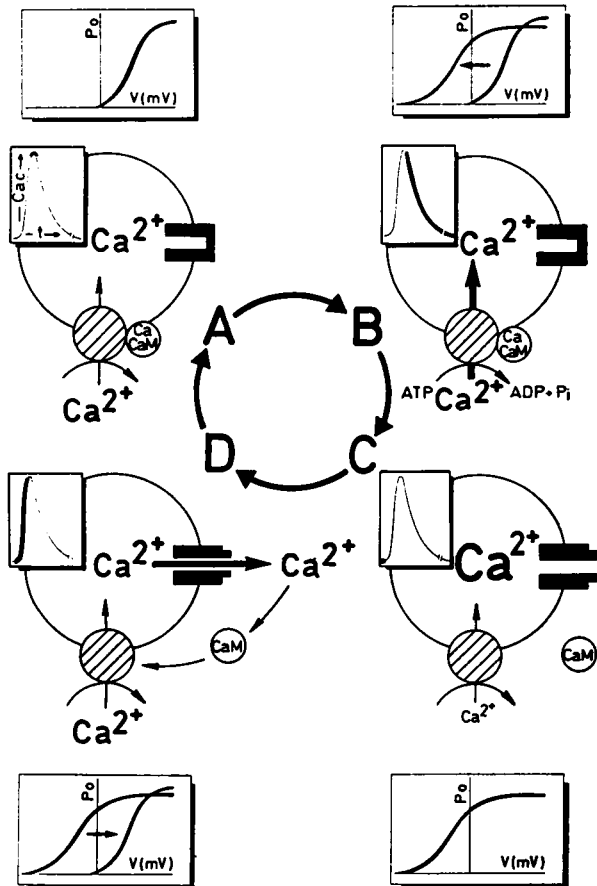
Fig. 5. Model for the Ca^{2+} oscillator proposed to comprise two components, the calmodulin-dependent Ca^{2+}-ATPase and BCC1 in the ER from *B.dioica* tendrils. In this model, the shifting of the gating voltage of BCC1 is dependent on the chemical potential difference of calcium across the ER membrane built up by the activity of the Ca^{2+} pump. Note that a transmembrane electrical potential difference is not required in this model and, consistent with experimental values, is assumed to be near zero. Cac, cytoplasmic free calcium; *t*, time; CaM, calmodulin; Ca CaM, calcium calmodulin complex. Capital letters refer to the phases of the calcium oscillation mentioned in the text.

been decreased as a consequence of previous channel opening events, which at the same time increased the level of cytoplasmic free Ca^{2+}, $[Ca^{2+}]_{cyt}$. Under now nearly symmetrical conditions, according to Figure 3C, the gating voltage $V_{1/2}$ for Ca^{2+} channel activation is significantly positive, which keeps the channels closed (phase A of the model). High $[Ca^{2+}]_{cyt}$ will activate—via calmodulin (Liß and Weiler, 1994)—the Ca^{2+}-ATPase, which will return $[Ca^{2+}]_{cyt}$ to its low resting level. Consequently (i) $[Ca^{2+}]_{lum}$ increases thus creating a large Ca^{2+} gradient across the ER membrane and (ii) $V_{1/2}$ is shifted along the voltage axis towards more negative membrane voltages (phase B, slow loading process). When a sufficiently high Ca^{2+} gradient is established and $V_{1/2}$ passes the actual value of membrane voltage, Ca^{2+} channels open (phase C). Immediately, Ca^{2+} permeates into the cytoplasm, thereby increasing $[Ca^{2+}]_{cyt}$ and decreasing $[Ca^{2+}]_{lum}$ (phase D, fast release process). Simultaneously, $V_{1/2}$ is shifted back to more positive voltages and phase A is reached again (Figure 5). It has been calculated that for a range of physiological parameters, if considered constant, bi-component oscil-

lators are fairly stable, even when large counter-ion fluxes (K^+ and/or Mg^{2+}, which are relevant for plant cells) are taken into account (Jafri and Gillo, 1994). Even though the membrane potential may also oscillate, the absolute differences predicted by the model are modest (between 5 and 20 mV; Jafri and Gillo, 1994), and this would not cause large differences in the open-state probability of BCC1. Gating voltage shifting driven by the *trans* ER chemical potential difference of Ca^{2+} can therefore be considered the dominant factor governing BCC1 activity.

Thus, the completely homeostatic cell, or part of it, should produce autonomous Ca^{2+} spikes with a certain frequency. Any factor impinging on this balance, at the level of the pump or the channel, through extra delivery of calcium from the apoplast or the vacuole or through calcium buffering in the cytoplasm, should interfere with this process. The mechanism by which the tendril recognizes a sliding surface, i.e. a dynamic spatial and temporal pattern of touch, may thus involve the modulation of Ca^{2+} spiking. It has been pointed out (Tsien and Tsien, 1990), and indeed reported for many excitable and even non-excitable animal cells (e.g. Petersen *et al.*, 1993), that frequency-encoded calcium signaling (i) improves the signal-to-noise ratio, (ii) improves the spatial resolution of a signal, and (iii) allows a smoothly graded input; all, in fact, are important parameters for a tendril establishing contact with a supportive structure. Alternatively (or additionally), BCC1 may serve to regulate the concentration of calcium in the ER lumen which is probably critical for ER function.

In conclusion, our findings provide direct evidence for the existence of regulated calcium release channels in the ER of higher plants. Their characteristics suggest them to respond to the transmembrane Ca^{2+} gradient within expected physiological ranges. Thus, these channels could be important elements in cellular calcium signaling in higher plants. The occurrence of similar channels in other organs and other plant species needs to be investigated to gain a deeper understanding of ER calcium channels and their physiological roles in higher plants.

Materials and methods

Biochemical and physiological techniques

HEPES–KOH, 1 mM DTT, 3 mM MgSO$_4$, pH 7.1, and was centrifuged at 110 000 g and 4°C for 2.5 h using a Kontron TST 28.38 swinging bucket rotor. Fractions (1 ml) were collected.

The fractions from 32 to 40% sucrose (1.135–1.175 g/cm^3) contained the rough ER contaminated with plasma membrane and broken plastids. From this material, the rough ER was purified further by an ethylene diamine tetraacetic acid (EDTA)-dependent density shift technique as follows. The pooled fractions from a 32 to 40% sucrose interface from two gradients were diluted with one volume of 5 mM HEPES–KOH (pH 7.1) containing 6% (w/w) sucrose, 1 mM DTT and 3 mM EDTA and centrifuged. The sediments were resuspended in the same buffer containing 0.5 mM PMSF and 50 µg/ml chymostatin and layered as a 2 ml aliquot on top of a sucrose gradient with MgSO$_4$ replaced by 3 mM EDTA. After centrifugation (110 000 g, 4°C, 2.5 h, TST 28.38 rotor), the ER, now shifted to a density range of 1.085–1.130 g/cm^3 (21–30% sucrose) due to the loss of ribosomes and thus separated from contaminating membranes, was collected, diluted with one volume of 25 mM HEPES–KOH (pH 7.2) containing 0.25 M sucrose and 6 mM MgSO$_4$, and repelleted at 265 000 g. This material is hereafter referred to as ER. To prepare ER vesicles with intravesicular Gd^{3+}, the whole preparation was performed in the presence of 20 µM GdCl$_3$. The final preparations were resuspended at 0.5 mg protein/ml of 250 mM sucrose, 6 mM MgSO$_4$, 25 mM HEPES–KOH, pH 7.2. Contaminations with other cellular membranes in this preparation were undetectable. Notably, mitochondrial membranes, chloroplast membranes, plasmalemma and tonoplast were removed by the techniques employed (Liß and Weiler, 1994).

^{45}Ca^{2+} loading experiments were performed as reported previously (Liß and Weiler, 1994). The procedure loads selectively the 'right side-out' fraction of ER vesicles (with the cytoplasmic side of the membrane facing the incubation medium and the vesicle lumen corresponding to the ER lumen). In brief, all assays were performed at 25°C and 0.1 ml final assay volume. ER membranes (8 µg of protein, 10 µl) were added to 90 µl of assay medium [25 mM HEPES–KOH, pH 7.2, containing 0.25 M sucrose, 6 mM MgSO$_4$, 3 mM ATP, 15 µM [^{45}Ca]Cl$_2$ (67–130 MBq, 15–60 TBq/mol)], mixed and incubated for the times indicated (usually from 2 to 10 min). Controls were run in parallel without ATP. Reactions were terminated by adding 0.5 ml of stop buffer (assay medium without ATP and [^{45}Ca]Cl$_2$ but with added 1 mM EGTA), mixing and vacuum filtration over nitrocellulose membranes (0.45 µm; Schleicher & Schuell, Dassel, Germany). The filters were washed three times with 1 ml of stop buffer, then dried and counted after dissolution in 3 ml scintillation cocktail (Hydroluma; Baker Co., Deventer, The Netherlands) using a Phillips PW 4700 scintillation counter (window 0.4–1990 keV). Modifications of this protocol (data in Figure 1C) are detailed in the legend. The calculation of free calcium concentration was made with the program Chelator, written by Th.Schoenmakers, Nijmegen, The Netherlands.

Electrophysiological techniques

For reconstitution experiments (Boheim *et al.*, 1981; Hanke *et al.*, 1984), planar bilayers (Rink *et al.*, 1994) were prepared from a solution of 80 parts (w/w) 1-palmitoyl-2-oleoyl-glycero-3-phosphatidylcholine and 20 parts (w/w) 1,2-dioleoyl-glycero-3-phosphatidylethanolamine (Avanti Polar Lipids Inc., Alabaster, AL) dissolved in *n*-decane (15 mg/ml). ER vesicles (0.5–1.0 µg of protein) were added to the *cis* compartment. We define the *trans* compartment to be at ground potential. Thus, the value of the applied voltage is that of the electrode potential in the *cis* compartment, and a positive current (upward deflections) corresponds to cation transfer from *cis* to *trans*. Voltage values were corrected before starting each measurement for (i) electrode potential differences due to different chloride activities of the compartment electrolytes and (ii) electrode asymmetry potentials, which sum to 5–7 mV in the case of CaCl$_2$/KCl gradients and to 4–6 mV in the case of CaCl$_2$/(choline chloride plus CaCl$_2$) gradients, respectively. Activities (at 25°C) were taken from D'Ans and Lax (1967). Liquid junction potentials were not present in our planar bilayer experiments, because Ag/AgCl electrodes were inserted directly into the compartment electrolytes. To gain a reference orientation of the Ca^{2+} channel in the planar bilayer, we state that it opens at positive voltages. Experiments were carried out at 18°C using electrolytes buffered with 10 mM HEPES–KOH, pH 7.0. Current and capacitance measurements were carried out with a BLM-120 Membrane Amplifier (Biologic, Echirolles, France). The amplifier signal was filtered with a corner frequency of 1 kHz and recorded continuously on a DAT recorder (DTR-1204; Biologic). For data evaluation on an ATARI Mega ST-4, current tracks were digitized using an ITC-16 ST interface and software (Recorder) from Instrutech (Elmont, NY). We

chose a sample frequency of 10 kHz. Single-channel current amplitudes and open-state probabilities were analyzed using TAC (Instrutech). TAC uses the 50% threshold method for the detection of signals (Colquhoun and Sigworth, 1983). Curve fitting was performed with the Curalyse program written by Dr J.Ströttchen, Bochum, Germany.

Acknowledgements

References

Allen,G.J. and Sanders,D. (1994) *Plant Cell*, **6**, 685–694.

Boheim,G., Hanke,W., Barrantes,F.J., Eibl,H., Sakmann,B., Fels,G. and Maelicke,A. (1981) *Proc. Natl Acad. Sci. USA*, **78**, 3586–3590.

Braam,J. and Davis,R.W. (1990) *Cell*, **60**, 357–364.

Colquhoun,D. and Sigworth,F.J. (1983) In Neher,E. and Sakmann,B. (eds), *Single Channel Recording*. Plenum Press, New York, pp. 191–264.

D'Ans,J. and Lax,E. (1967) *Handbook for Chemists and Physicists*. Springer Verlag, Berlin, Germany.

Ding,J.P. and Pickard,B.G. (1993) *Plant J.*, **3**, 713–720.

Elinder,F. and Århem,P. (1994) *Biophys. J.*, **67**, 71–83.

Falkenstein,E., Groth,B., Mithöfer,A. and Weiler,E.W. (1991) *Planta*, **185**, 316–322.

Gilroy,S., Fricker,M.D., Read,N.D. and Trewavas,A.J. (1991) *Plant Cell*, **3**, 333–344.

Hanke,W., Boheim,G., Barhanin,J., Pauron,D. and Lazdunski,M. (1984) *EMBO J.*, **3**, 509–515.

Hille,B. (1992) *Ionic Channels of Excitable Membranes*. Sinauer, Sunderland, MA.

Jafri,M.S. and Gillo,B. (1994) *Cell Calcium*, **16**, 9–19.

Kendall,J.M., Dormer,R.L. and Campbell,A.K. (1992) *Biochem. Biophys. Res. Commun.*, **189**, 1008–1016.

Knight,M.R., Campbell,A.K., Smith,S.M. and Trewavas,A.J. (1991) *Nature*, **352**, 524–526.

Knight,M.R., Smith,S.M. and Trewavas,A.J. (1992) *Proc. Natl Acad. Sci. USA*, **89**, 4967–4971.

Lacampagne,A., Gannier,F., Argibay,J., Garnier,D. and LeGuennec,J.Y. (1994) *Biochim. Biophys. Acta*, **1191**, 205–208.

Lee,K.S. and Tsien,R.W. (1984) *J. Physiol.*, **354**, 253–272.

Leonard,R.T. and Hepler,P.K. (1990) *Calcium in Plant Growth and Development. Current Topics in Plant Physiology*. American Society of Plant Physiologists, Rockville, MD, Vol. 4.

Liß,H. and Weiler,E.W. (1994) *Planta*, **194**, 169–180.

Meissner,G. (1983) *Mol. Cell. Biochem.*, **55**, 65–82.

Pantoja,O., Gelli,A. and Blumwald,E. (1992) *Science*, **255**, 1567–1570.

Petersen,C.C.H., Petersen,O.H. and Berridge,M.J. (1993) *J. Biol. Chem.*, **268**, 22262–22264.

Ping,Z., Yabe,I. and Muto,S. (1992) *Biochim. Biophys. Acta*, **1112**, 287–290.

Rink,T., Bartel,H., Jung,G., Bannwarth,W. and Boheim,G. (1994) *Eur. Biophys. J.*, **23**, 155–165.

Schroeder,J.I. and Hagiwara,S. (1990) *Proc. Natl Acad. Sci. USA*, **87**, 9305–9309.

Stephenson,D.G., Wendt,I.R. and Forrest,Q.G. (1981) *Nature*, **289**, 690–692.

Thuleau,P., Ward,J.M., Ranjeva,R. and Schroeder,J.I. (1994) *EMBO J.*, **13**, 2970–2975.

Tsien,R.W. and Tsien,R.Y. (1990) *Annu. Rev. Cell Biol.*, **6**, 715–760.

Ward,J.M. and Schroeder,J.I. (1994) *Plant Cell*, **6**, 669–683.

Weiler,E.W., Albrecht,T., Groth,B., Xia,Z.-Q., Luxem,M., Liß,H., Andert,L. and Spengler,P. (1993) *Phytochemistry*, **32**, 591–600.

Weiler,E.W., Kutchan,T.M., Gorba,T., Brodschelm,W., Niesel,U. and Bublitz,F. (1994) *FEBS Lett.*, **345**, 9–13.

Yang,X.-C. and Sachs,F. (1989) *Science*, **243**, 1068–1071.